66 | März 1960

SCHRIFTENREIHE SCHIFFBAU

K. Hasselmann

Decay of Wave-Induced Velocity Fluctuations in the Small HSVA Tank

TUHH
Technische Universität Hamburg-Harburg

INSTITUT FÜR SCHIFFBAU DER UNIVERSITÄT HAMBURG
Prof. Dr.-Ing. G. Weinblum

Decay of Wave-Induced Velocity Fluctuations in the Small HSVA Tank.

K. Hasselmann

Hamburg, März 1960

INSTITUT FÜR SCHIFFBAU DER UNIVERSITÄT HAMBURG
Prof. Dr.-Ing. G. Weinblum

Decay of Wave-Induced Velocity Fluctuations in the Small HSVA Model Basin.

K. Hasselmann

1) Object and Method of Investigation. The measurements described below are the first part of an intended general investigation of the decay of velocity fluctuations generated by towing models in a model basin. The fluctuations consist of two components, generally of comparable magnitude: a wave component, which rapidly disperses its energy uniformly over the surface of the basin and decays primarly through energy loss by reflection at the walls, and a turbulent component generated in the model wake, which diffuses more slowly and decays locally through the combined action of inertia and viscous forces. Both components will probably have a comparable influence on the stimulation of boundary-layer transition.

In order to measure very low fluctuation intensities during as long a period as possible it was decided to operate the hot wires in the most sensitive region of their calibration curves, i.e. at rest. This resulted in a transformation of the normal energy spectrum measured with a wire moving with the model (fig. 1) into a spectrum of the type schown in fig.2. In fig. 1 the turbulent frequencies are of the order $\frac{U_o}{L}$ (U_o = towing velocity, L = turbulence scale), where as the frequency of the wave component is zero or twice the natural frequency $\nu_o = \frac{g}{2\pi U_o}$ (after an uneven number of reflections at the end-walls of the basin - it has been assumed for simplicity of discussion that the main wave energy lies in the wave train travelling in the direction of the model astern). In fig. 2

the turbulence frequencies are of the much smaller order $\frac{U_1}{L}$ (U_1 = wake velocity), where as all wave components have frequencies near ν_o. Measuring with a stationary hot wire thus has the additional advantage of enabling easy separation of the wave and turbulence components of the velocity fluctuations. Fig. 3 is a typical oscillograph record showing the periodic wave component superimposed on more slowly varying turbulence fluctuations. The mean square values of the wave component obtained from the records were subject to some statistical scatter, as the random fluctuations of the envelop were rather slow (due to the narrow band width of the wave spectrum). It was not possible to gain more than a very rough estimate of the mean intensities of the turbulence component from the records, as the turbulence fluctuation periods measured with a stationary hot wire are of the same order of magnitude as the decay time. In general, the turbulence and wave components were found to be of comparable magnitude.

2) Experimental Arrangement. The measurements were carried out in the small towing tank of the HSVA (Hamburgische Schiffbau Versuchsanstalt). The dimensions of the tank and the position of the measuring station P are shown in fig. 4. The decay times were measured from the instant the model passed the point P. At the end of the run, the model was released and the carriage returned to the measuring station.

The hot wire apparatus was of the constant-current type. The hot wire constituted one arm of a Wheatstone bridge, the out-of-balance of which was amplified with a transistor DC-amplifier and fed to a galvanometer recorder. The film records were of 10 to 40 seconds duration and in one- to two-minute intervals

3) Calibration. As the velocity fluctuations recorded by the hot wire were about a very small mean value (the wake velocity), a special apparatus was required to calibrate the wire at low velocities. Fig. 5 showing the method of operation should be self-explanatory. From the amplitudes of the periodic records abtained for different angular velocities of the driving disc D, calibration curves relating the flow velocity directly to the final instrument reading were obtained (fig. 6). In the actual fluctuation measurements, the mean wake velocity determining the "working point" on the calibration curves were measured by stopping the time taken by particles on the surface to traverse a fixed distance.

4) Results. The decay of the wave-induced velocity fluctuations were measured at several depths after runs with two models of different size, each at two speeds:

	L_{pp} [m]	B [m]	D [m]	C_B	∇ [dm^3]	Velocities (Froude Nrs.) [m/s]	
Model 1	1,22	0,17	0,062	0,146	9,56	0,65 (0,188)	0,9 (0,260)
Model 2	2,766	0,366	0,153	0,761	118,45	1,0 (0,192)	1,5 (0,288)

The results are shown in figs. 7, 8 and 9. u'_w is the root mean square value of the wave-induced fluctuation. The maxima and minima of the decay curves are due to successive reflections of the wave train at the end walls of the basin. The intensities of the wave component decay to less than 0,01 % of the towing velocity within 3 to 8 minutes. At this value of the fluctuation intensity the water surface already appeared practically calm. The hot wire still detected small

intermittent wave fluctuations for decay times up to 12 minutes. The minimum intensity of about 0,1 % generally assumed to be still capable of affecting boundary-layer transition on a flat plate is attained after a relatively short time of 2 minutes for model 1 and 5 minutes for model 2. The general practice of waiting until the water surface is practically calm before making the next run is thus well on the safe side as regards the influence of the wave-induced velocity fluctuations on boundary-layer transition.

Original Oscillograph Record

Sold out

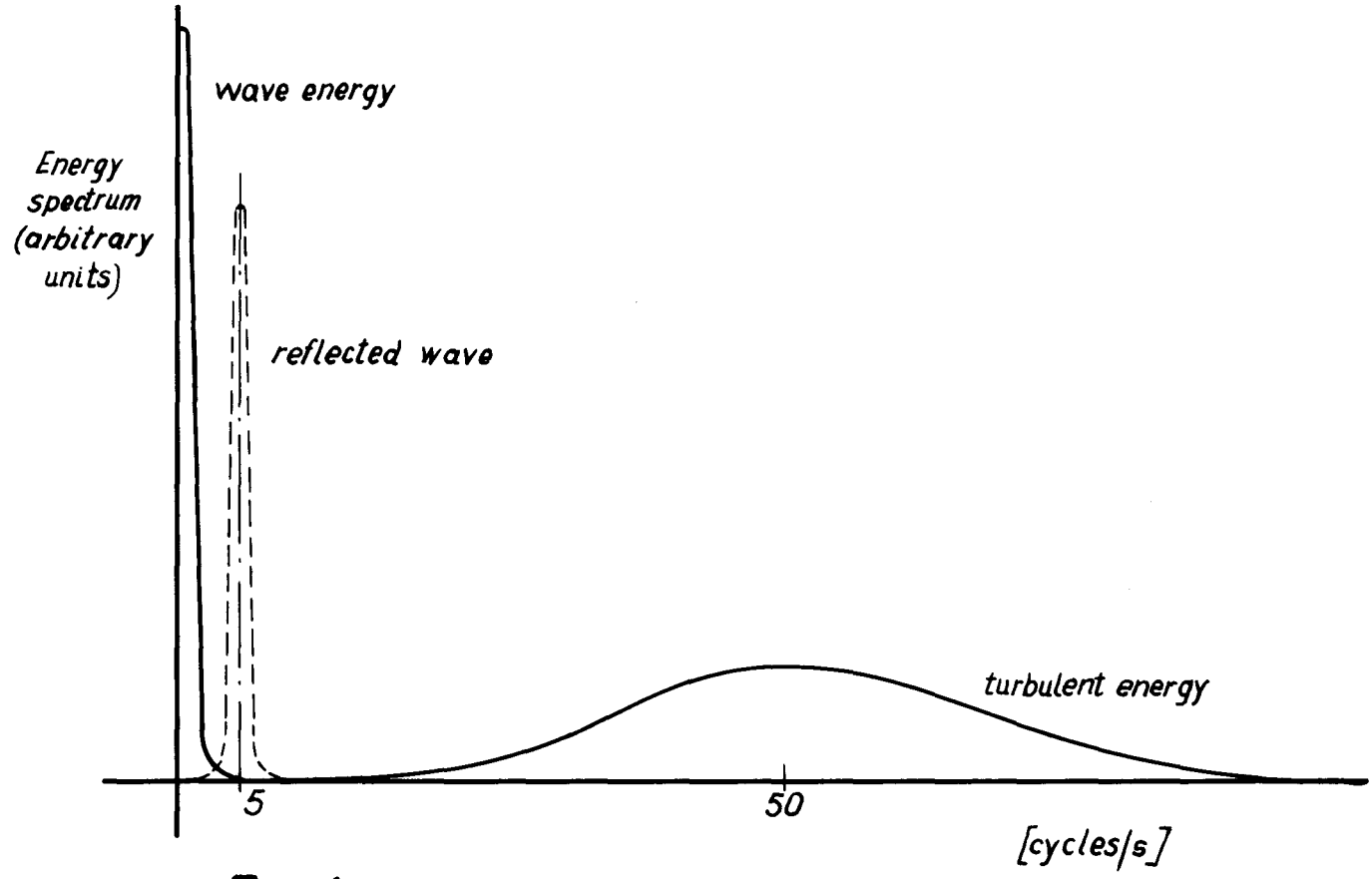

Fig. 1 Energy spectrum, probe moving with model

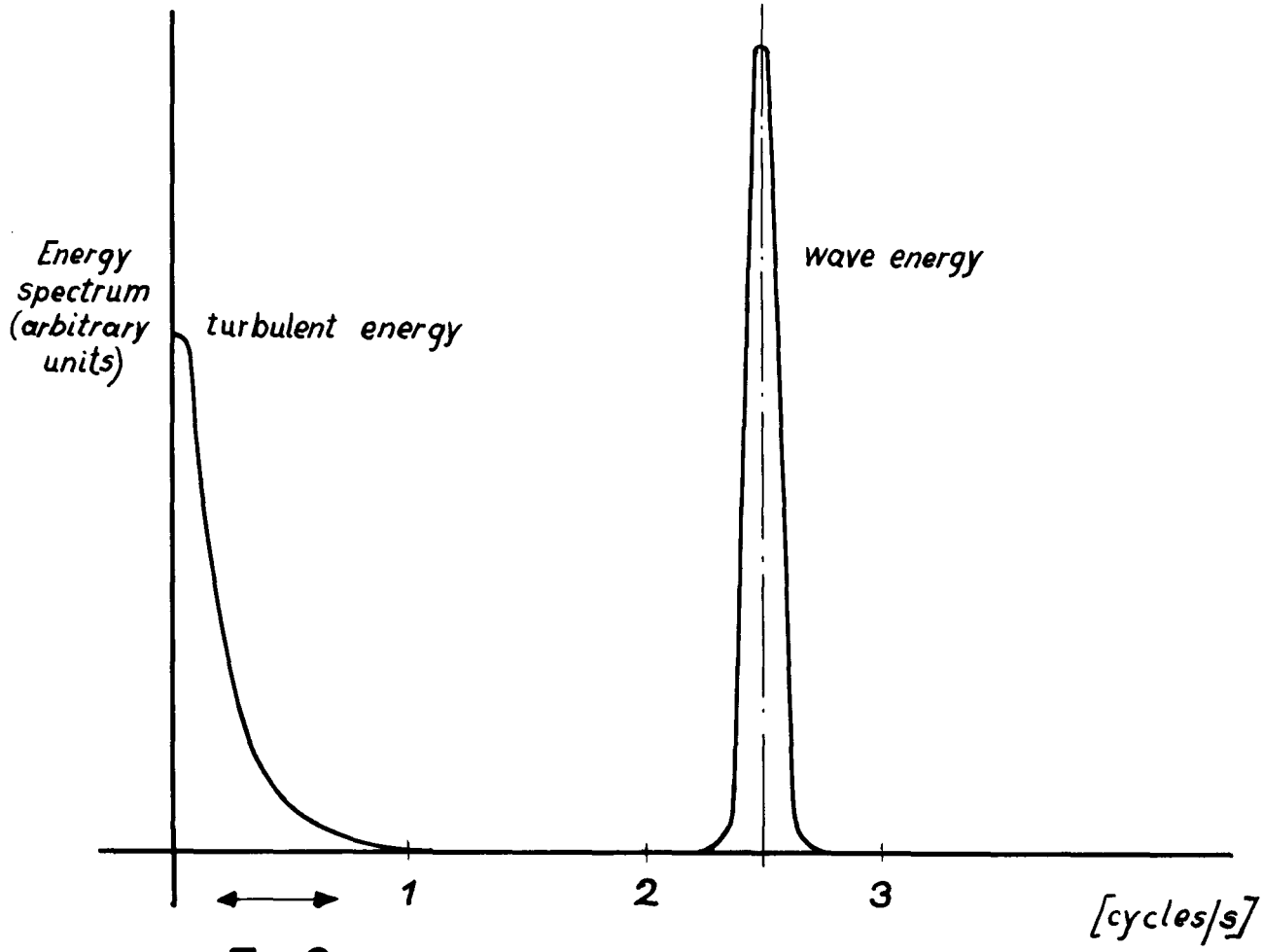

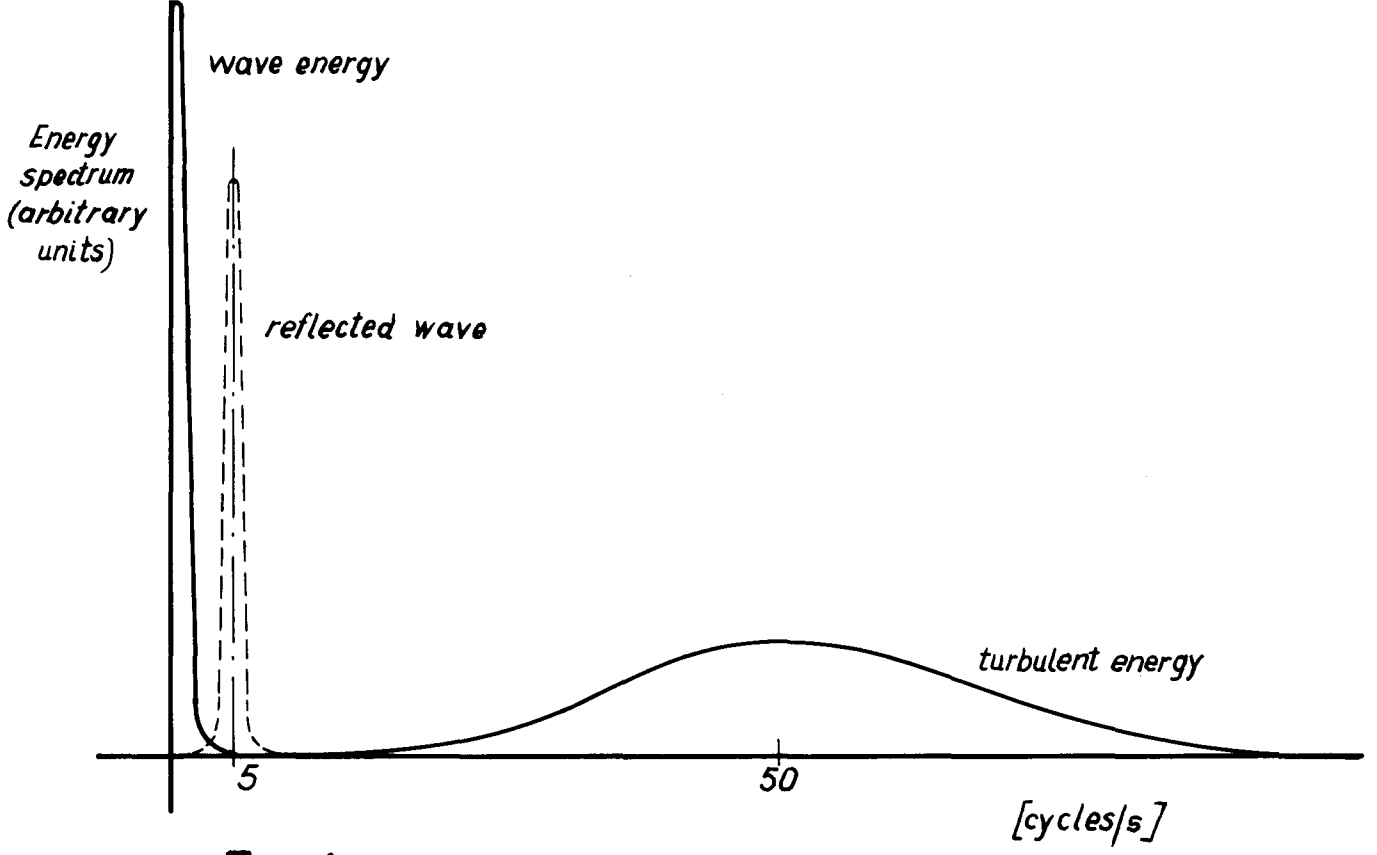

Fig. 1 Energy spectrum, probe moving with model

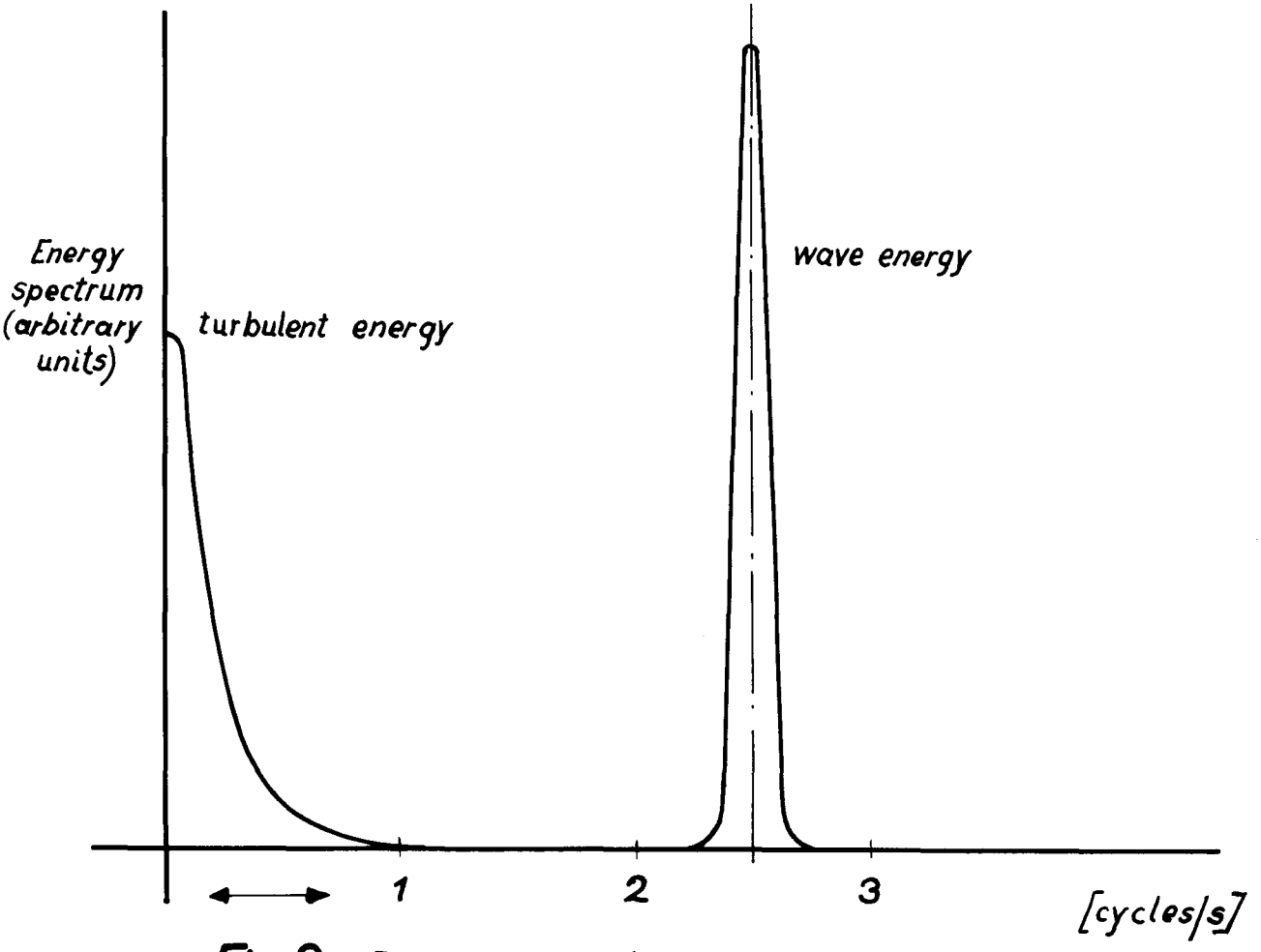

Fig. 2 Energy spectrum, probe stationary

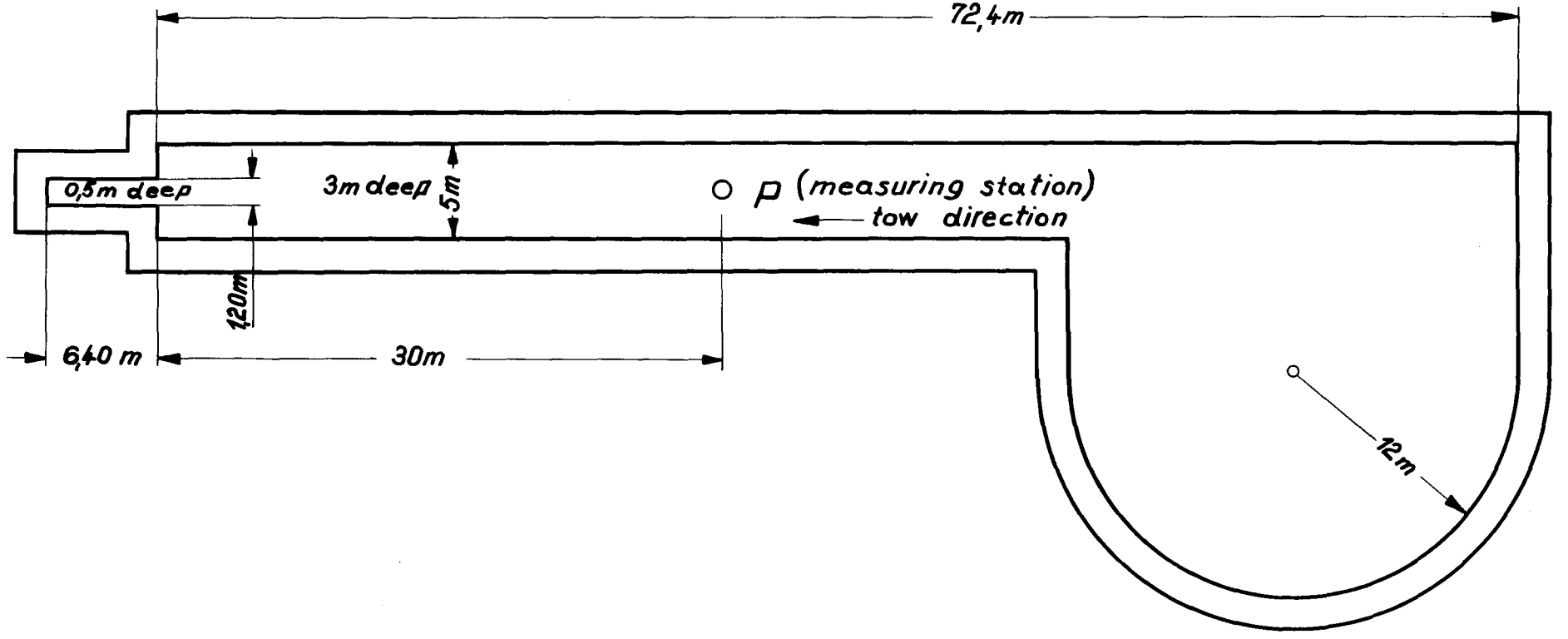

fig.4

The small HSVA model basin

Fig. 5

Hot wire calibrating apparatus

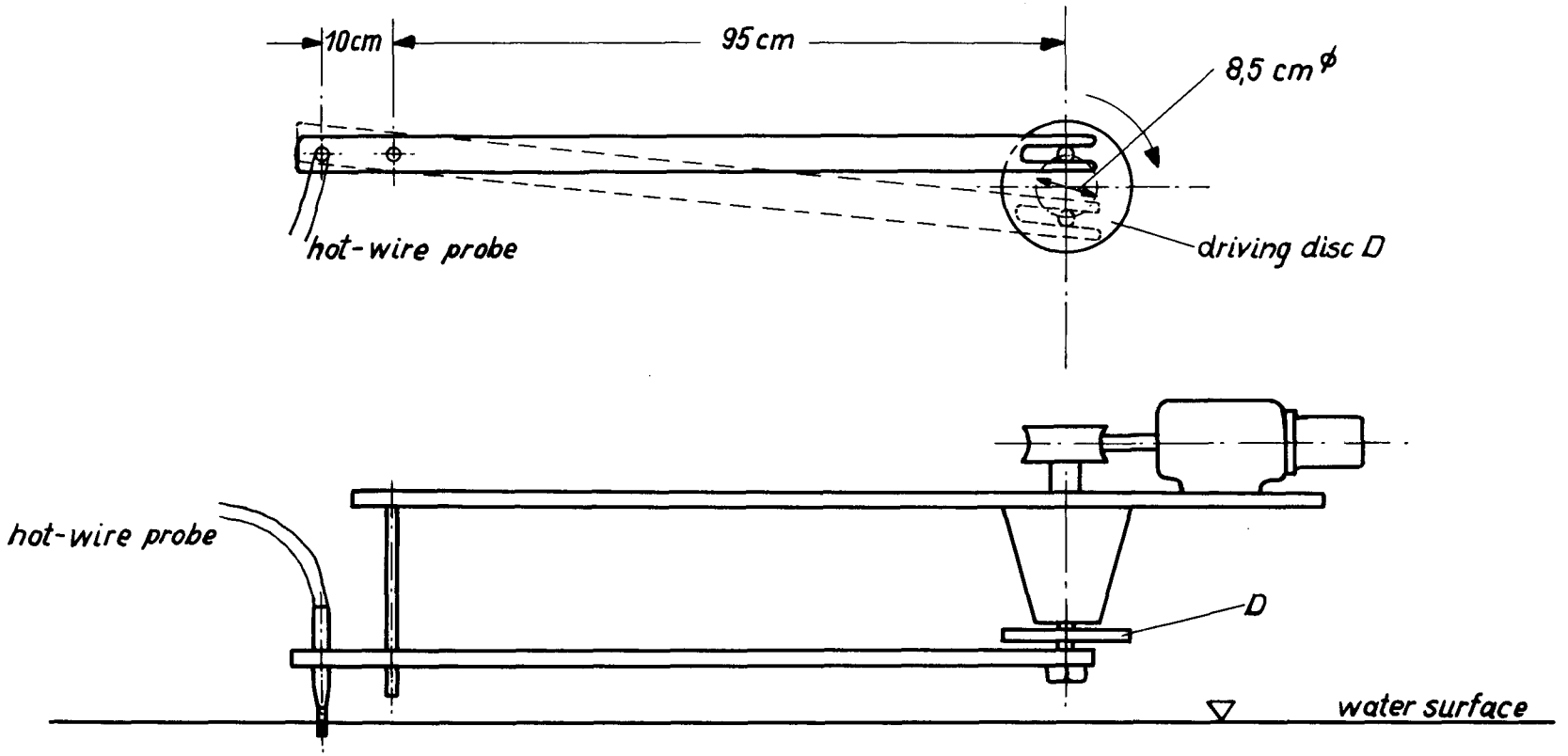

Fig. 6 Hot-wire calibration

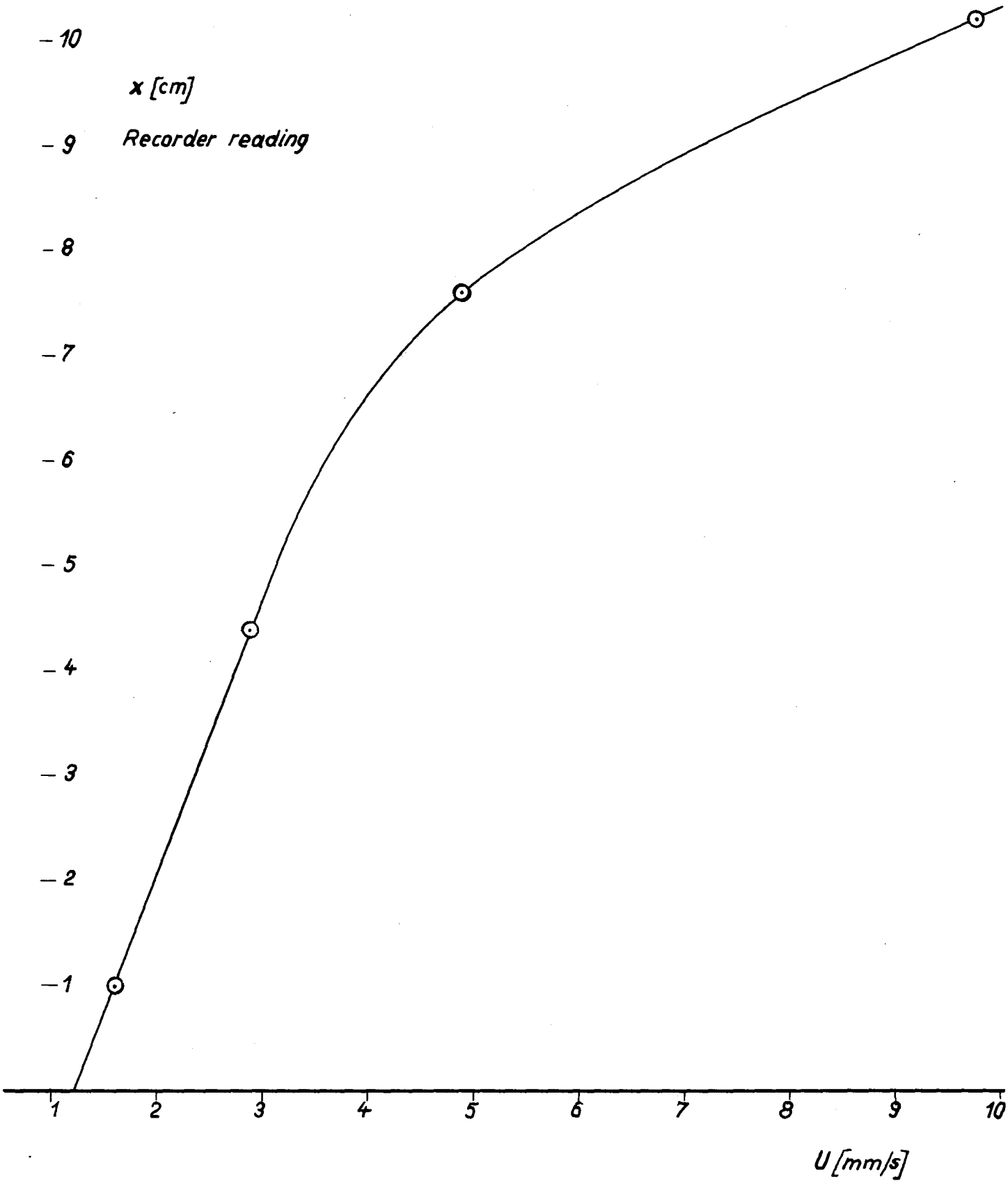

fig. 7

Model 1

$\frac{u'_\omega}{u_0}$ [%]

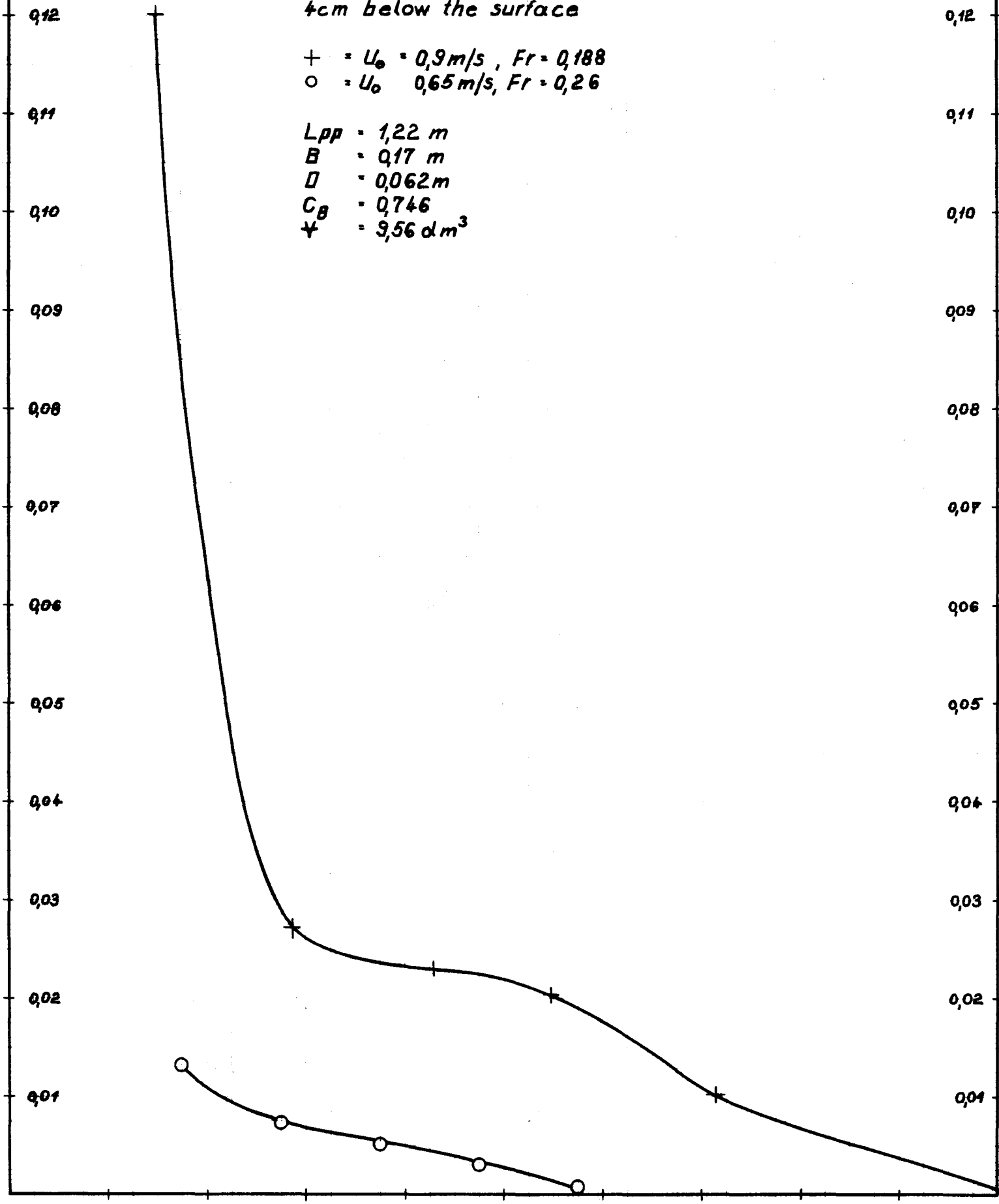

fig. 8

Model 2

U_o = 1 m/s , Fr = 0,192

\+ 4cm below the surface
× 23cm " " "

L_{pp} = 2,766m
B = 0,366m
D = 0,153 m
C_B = 0,761
∇ = 118,45 dm^3

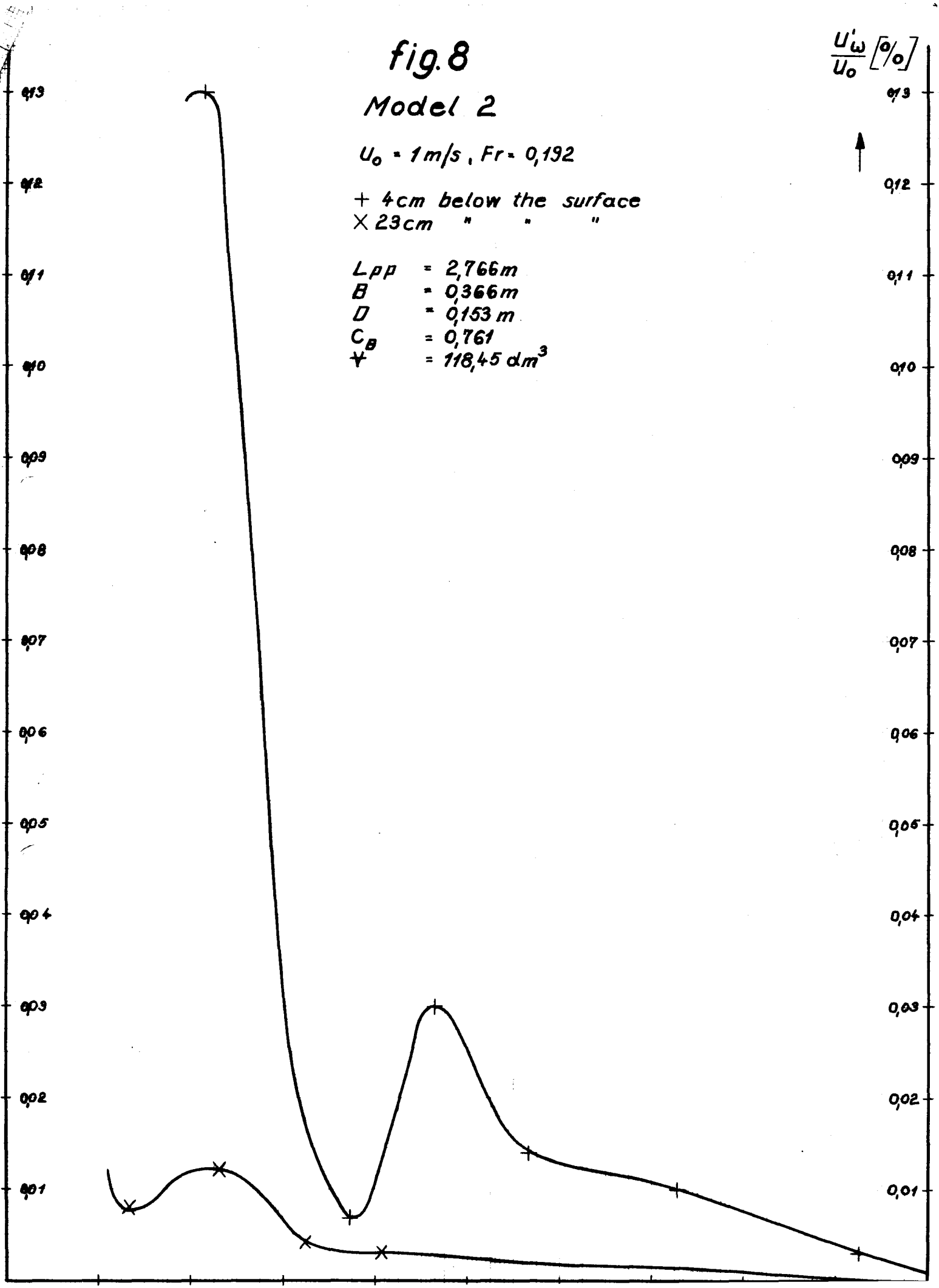

fig. 8

Model 2

U_o = 1 m/s , Fr = 0,192

\+ 4cm below the surface
× 23cm " " "

L_{pp} = 2,766m
B = 0,366m
D = 0,153 m
C_B = 0,761
∇ = 118,45 dm^3

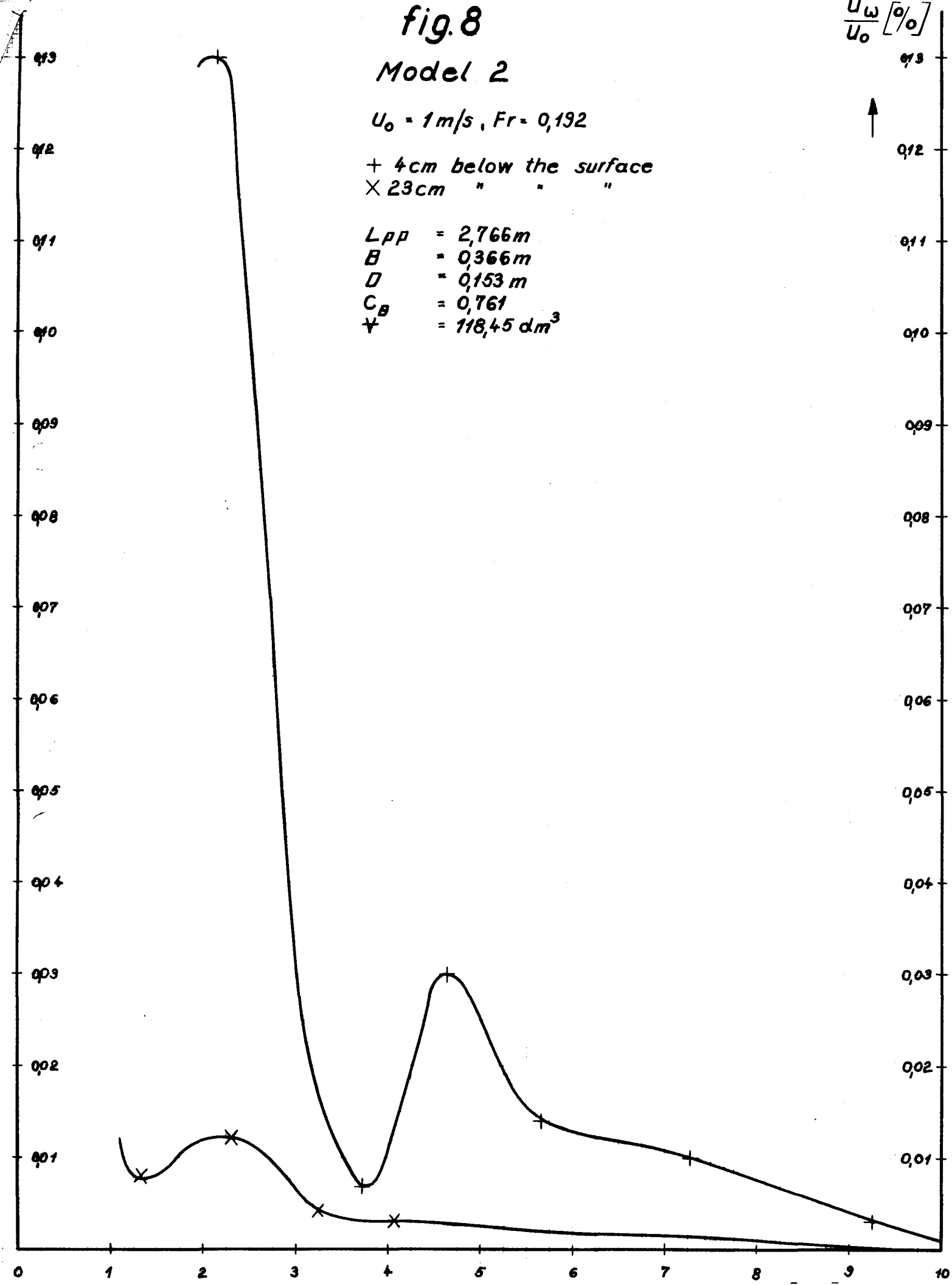

Fig. 3

Model 2

u_0 = 1,5 m/s , Fr = 0,288

$\frac{u'_\omega}{u_0}$ [%]

+ 4 cm below the surface
○ 13 cm " " "
× 23 cm " " "

L_{pp} = 2,766 m
B = 0,366 m
D = 0,153 m
C_B = 0,761
∇ = 118,45 dm³